

Simulation of temperature trends and thermal stresses on a monument under climate change conditions

Anna Antoniou^{1*}, Nicolas Moussiopoulos² and Nicolaos Theodossiou³

¹Mechanical Engineering Department, Aristotle University of Thessaloniki, GR 54124, Thessaloniki, Greece

²Aristotle University of Thessaloniki, GR 54124, Thessaloniki, Greece

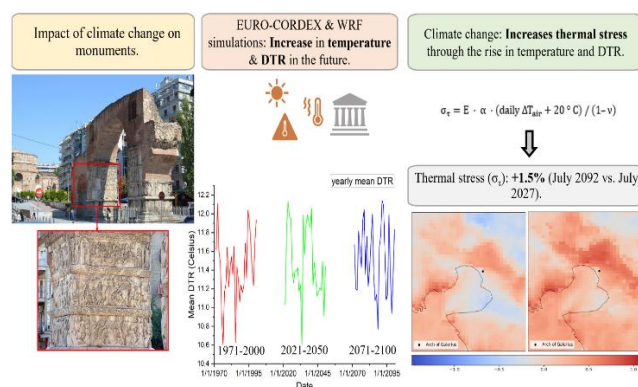
³Civil Engineering Department, Aristotle University of Thessaloniki, GR 54124, Thessaloniki, Greece

Received: 31/12/2024, Accepted: 10/05/2025, Available online: 04/06/2025

*to whom all correspondence should be addressed: e-mail: annaantoniou@meng.auth.gr

<https://doi.org/10.30955/gnj.07237>

Graphical abstract



Abstract

Climate change affects temperature and its variability, creating increased thermal stress on the materials of monuments located outdoors. This study investigates future temperature trends and their impact on the marble of the Triumphal Arch of Galerius in Thessaloniki, Greece, using data from the Coordinated Downscaling Experiment for European Domain (EURO-CORDEX) under the Representative Concentration Pathway 4.5 (RCP4.5) emissions scenario. The analysis compares the past period (1971–2000) with two future periods (2021–2050, 2071–2100), confirming the increase in temperature and temperature variability. High-resolution simulations (up to 1 km) of selected critical summer periods were conducted using the Weather Research and Forecasting model (WRF-ARW). The results show an increase in the number of days with significant temperature fluctuations, leading to higher thermal stress on marble. For example, during July 2092, there was an estimated 1.5% increase in thermal stress compared to July 2027. These findings highlight the importance of combining high-resolution climate simulations, future trends assessments, and analyses of climate-related impacts on structural materials. Such an approach is essential for preserving and protecting cultural heritage monuments under changing climate conditions.

Keywords: EURO-CORDEX, high-resolution simulations, temperature extremes, thermal variability, cultural heritage, marble weathering

1. Introduction

Climate change affects cultural heritage, posing significant challenges for its preservation and protection. Shifts in environmental factors, such as temperature, play a critical role in the maintenance and longevity of materials constituting monuments and cultural assets (Sesana *et al.*, 2020). Rising temperatures and changes in temperature variability have been documented as key drivers of increased thermal stress on materials (Koch and Siegesmund, 2004; Siegesmund *et al.*, 2021). According to Bonazza *et al.* (2009), the most notable change observed over this century is a general increase in the risk of thermal stress across the Mediterranean and Europe, making it essential to incorporate climate forecasts into cultural heritage conservation strategies.

Projected temperature increases due to climate change are expected to significantly heighten thermal stress on marble, especially in Mediterranean regions, where over 300 thermal stress events per year are anticipated in the future (Bonazza *et al.*, 2009). Monuments made of marble will be especially vulnerable, particularly in areas with a high density of such monuments, such as Greece (Bonazza *et al.*, 2009). Damage to calcite marble is linked to temperature fluctuations and the microstructural changes they induce, underscoring the need to understand these mechanisms in order to develop effective conservation strategies (Sassoni and Franzoni, 2014; Siegesmund *et al.*, 2021).

Although future climate impacts have been assessed in numerous studies – either specifically for materials such as marble (Bonazza *et al.*, 2009), or more broadly for heritage sites (Tringa and Tolika, 2023) – most of these analyses are constrained by lower spatial resolutions. Recent advances, such as those demonstrated in studies integrating high-resolution meteorological data into smart city services (Surendran *et al.*, 2021) and in deep learning models for wind speed (Surendran *et al.*, 2023) and long-

term rainfall prediction (Subramanian *et al.*, 2024) illustrate the benefits of employing fine-scale data and sophisticated modeling techniques to capture local climatic variability. These examples underscore the potential of downscaling approaches to significantly enhance our understanding of microclimatic effects in regions with complex geographical features. High-resolution approaches (e.g., 1 km) are crucial for understanding local microclimatic effects, especially in regions with complex geographical features and rich cultural heritage like Greece (Politi *et al.*, 2018; Tringa and Tolika, 2023). Recent studies, such as Ascenso *et al.* (2024), underscore the importance of downscaling for assessing the local impacts of climate change, although such approaches remain limited. Moreover, the relationship between climate parameters and their effects on monument materials has not been extensively investigated, despite its importance (Bonazza *et al.*, 2009).

Climate change alters parameters such as temperature, exerting increasing stress on outdoor monuments, which now face more adverse conditions. The motivation for this work lies in the pressing need to protect vulnerable heritage monuments from escalating thermal stress through refined climate projections. The present study aims to combine (1) an analysis of future climate trends, (2) high-resolution spatial and temporal modeling of climate variables through atmospheric models, and (3) an examination of how these changes affect structural materials - focusing on the calcite marble of an archaeological monument that has stood in Thessaloniki for 1,700 years. Accordingly, our key objectives are to (1) quantify how projected temperature variability intensifies thermal stress on calcite marble, (2) apply downscaling techniques for high-resolution (1 km) climate modeling in Greece, and (3) link specific climate parameters to the microstructural damage mechanisms of marble. Through these steps, we estimate the future thermal stress on the monument's materials, providing critical quantitative information for shaping strategies aimed at minimizing the impacts of climate change on cultural heritage monuments. The scope of our analysis focuses on Thessaloniki's iconic marble heritage, offering a blueprint for broader conservation efforts in regions with similar climatic and cultural conditions. By enhancing the spatial and temporal resolution of climate models, we create a more accurate framework for understanding how climate change threatens cultural assets and for designing effective protection strategies.

2. Materials and methods

2.1. Monument and material of study

The Triumphal Arch of Galerius is one of the most characteristic monuments of Thessaloniki (**Figure 1**). Built around 303 AD, it was dedicated to Galerius and the four emperors of the Tetrarchy (political system established by the Roman emperor Diocletian in the late 3rd century AD). The monument, recognized for its artistic and political significance, is part of the Galerian Complex, which also includes other notable structures such as the Rotunda and the Hippodrome. It was originally part of the emperor's

palace and features marble reliefs depicting Galerius's victorious campaigns against the Persian king Narses (Rees, 1993).



Figure 1. Map of Greece indicating the location of the Arch of Galerius, a photograph of the monument from the southwest, and a focus on its marble decoration

In this study, we examine the marble used in the monument. This marble is coarse-grained, with visible crystals, and consists almost entirely (over 99%) of calcite (Samara *et al.*, 2020). Although the monument is considered the best preserved of its kind from this era in Europe, it has suffered considerable damage, particularly in its marble sculptural decorations. Calcite marble is highly sensitive to environmental changes, so temperature fluctuations can accelerate its deterioration (Sassoni and Franzoni, 2014). The interior shows signs of intracrystalline decomposition, increased porosity, and disrupted internal cohesion (Samara *et al.*, 2020).

Temperature plays a crucial role in the microstructure and grain growth of calcite marble, with higher temperatures leading to larger grains (Covey-Crump and Rutter, 1989) – a condition that worsens the marble's state. The material is porous and contains calcite crystals of diverse sizes, ranging from fine grains (0.3–1.5 mm) to larger ones (2–4 mm); smaller crystals fill the gaps, forming a dense structure (Samara *et al.*, 2020). However, its coarse-grained nature makes it more prone to decay because large calcite crystals create discontinuities and microcracks (diameter < 10 μ m), accelerating the decomposition process and increasing its vulnerability to external factors (Samara *et al.*, 2020).

Rising temperatures further increase porosity through thermal expansion and the formation of microcracks (Luque *et al.*, 2011). In fact, on building facades in many European countries – where summer temperatures range between 40–50 °C– calcite marbles exhibit higher porosity and more microcracks (Malaga-Starzec *et al.*, 2002). Such materials, once more porous, have lower mechanical strength and are more susceptible to cracking and bending (Malaga-Starzec *et al.*, 2002). Overall, the marble's structure, porous nature, and microcracks make it vulnerable to physical and chemical weathering, leading to further deterioration of its condition.

2.2. Methodology and objective

The methodology followed in this study consists of the following steps: First, future temperature trends were estimated using EURO-CORDEX data (Jacob *et al.*, 2020)

under the RCP4.5 scenario, applying both the climate indices developed by the Expert Team on Climate Change Detection and Indices (ETCCDI) (Zhang *et al.*, 2011) and basic statistical indicators. Statistical analysis was then performed to estimate the mean monthly temperature range, to select the most critical future months in terms of increased temperature fluctuations. Following this, a dynamical downscaling method using the WRF model (Skamarock *et al.*, 2019) was performed for these critical summer months, enabling the estimation of temperature at a resolution up to 1 km. Finally, the high-resolution temperature variability outputs from the WRF model were used in an equation that calculates thermal stress in calcite marbles, thus assessing the impact of future temperature changes (due to climate change) on marble materials.

2.3. Method of estimating climate trends

This work focuses on assessing changes in temperature. The study of temperature trends was conducted for three 30-year periods: the historical period (1971-2000, baseline), the near future period (2021-2050), and the far-future period (2071-2100), following Ioannidis *et al.*

Table 1: The climate indices used and their descriptions.

Indices	Description	Units
FD	number of days in a year where $\text{tasmin} < 0^\circ\text{C}$	days
ID	number of days where $\text{tasmax} < 0^\circ\text{C}$	days
TXx	monthly maximum value of daily maximum temperature (tasmax)	$^\circ\text{C}$
TNn	monthly minimum value of daily minimum temperature (tasmin)	$^\circ\text{C}$
DTR	annual mean of the daily differences between tasmax and tasmin	$^\circ\text{C}$

The above climate indices are combined with the following key statistical indicators to measure data dispersion.

Standard deviation (SD):

$$SD = \sqrt{\frac{1}{N} \sum_{i=1}^N (x_i - \bar{x})^2} \quad (1)$$

The SD measures how spread out the values are around the mean, indicating the average distance of the sample values from the mean. This provides insights into the variability of climate variables.

Interquartile Range (IQR):

$$IQR = Q_3 - Q_1 \quad (2)$$

The IQR is defined as the difference between the 75th percentile (Q_3) and the 25th percentile (Q_1), reflecting the range within which 50% of the data values lie. It is considered a robust measure of dispersion because it is less affected by extreme values than SD.

For the periods 2021–2050 and 2071–2100, a statistical analysis was conducted to identify which future months might experience an increased DTR, under the same climate scenario and with the same global and regional climate models used to estimate future trends. Specifically, the average monthly variability was calculated for each month of these future periods rather than the maximum variability, since the focus was on finding the

(2024). Initially, climate data were obtained from EURO-CORDEX (<https://euro-cordex.net/060378/index.php.en>) under the RCP4.5 climate scenario (Thomson *et al.*, 2011). The RCP4.5 scenario represents a middle-range scenario regarding emissions and radiative forcing (van Vuuren *et al.*, 2011), where radiative forcing stabilizes at 4.5 W m^{-2} relative to pre-industrial levels by the year 2100, without exceeding this value.

The EURO-CORDEX climate data used in this study have a spatial resolution of 0.11° ($\sim 12.5 \text{ km}$) and daily temporal resolution. The Global Circulation Model (GCM) is based on MPI-MMPI-ESM-LR (Stevens *et al.*, 2013), while the Regional Climate Model (RCM) is the downscaled RCA4 model. Some indices developed by the ETCCDI were employed, focusing on moderate weather phenomena that occur regularly during a typical year. Data processing – specifically the statistical analysis focusing on the geographical area of Thessaloniki while maintaining the original spatial analysis of EURO-CORDEX was conducted using the CDO library (Schulzweida, 2023). Table 1 presents the ETCCDI indices used in this study.

months with the largest number of days showing relatively high variability, rather than a single extreme high variability event on one or a few days. Based on this statistical analysis, the selected future periods were June 2023, July 2027, June 2048, July 2050, July 2077, and July 2092.

2.4. Dynamical downscaling method

The model used for both past and future simulations was WRF-ARW (Version 4.4, September 2024). WRF is a non-hydrostatic, open-source mesoscale model developed by the National Center for Atmospheric Research. The model is applied when higher-resolution simulations are required, using the dynamical downscaling method. Thus, starting from the resolution of General Circulation Models (GCMs), we can achieve the finer resolution of Regional Climate Models (RCMs), especially when studying phenomena at the local scale.

The grids used for the future simulations are shown in **Figure 2**, while different grids were employed for the historical simulations (**Table 2**) because the input data were of higher resolution, making the 27 km grid unnecessary. As a result, the future simulations utilized four grids, whereas the historical simulations used three. WRF model simulations are based on the physical modeling of key phenomena in the troposphere and the lower stratosphere, with the corresponding equations solved numerically on a three-dimensional computational

grid. This approach requires substantial computational resources and involves processing large volumes of data. Therefore, the model simulations were conducted for short-term periods (future months rather than years) using a high-performance parallel computing system with remarkably high overall capacity (the BwUniCluster 2.0 supercomputing system).

The physical processes and parameterization schemes of the WRF model were selected based on previous climate simulations and sensitivity analyses conducted by other researchers in the Mediterranean region (Castorina *et al.*, 2022). All schemes and model configuration details are presented in **Table 2**.

Table 2. Summary of the model setup and input data for past and future climate simulations

Period	past	future
Input data	ERA5 Reanalysis	NCAR CESM Bias-Corrected CMIP5 Output
Input data sources	https://cds.climate.copernicus.eu/datasets/reanalysis-s-era5-pressure-levels?tab=overview (Hersbach <i>et al.</i> , 2023a) https://cds.climate.copernicus.eu/datasets/reanalysis-s-era5-single-levels?tab=overview (Hersbach <i>et al.</i> , 2023b)	https://data.ucar.edu/dataset/ncar-cesm-global-bias-corrected-cmip5-output-to-support-wrf-mpas-research (Monaghan <i>et al.</i> , 2014)
Horizontal resolution of input data	0.25 × 0.25	1 × 1
Interval of input data	6 hours	6 hours
Nesting	One-way nesting	
Domains	d01 (9 km, 485×257 cells) d02 (3 km, 475×247 cells) d03 (1 km, 463×235 cells)	d01 (27 km, 374×243 cells) d02 (9 km, 364×229 cells) d03 (3 km, 352×217 cells) d04 (1 km, 340×205 cells)
Map projection	Lambert Conformal	
Vertical layer	31	27
Geographic data resolution	30s	
Microphysics	Thompson scheme	
Longwave radiation	RRTMG scheme	
Shortwave radiation	RRTMG scheme	
Surface layer	MM5 scheme	
Land surface	Noah Unified model	
Planetary boundary layer	Mellor-Yamada-Janjic (MYJ) scheme	
Cumulus parameterization	Kain-Fritsch (new Eta) scheme	



Figure 2. The WRF grids for future simulations: d01 (27 km), d02 (9 km), d03 (3 km), and d04 (1 km)

2.5. Method of estimating thermal stress in marble

Thermal stress (σ_t), considering only temperature variations in the marble material, can be calculated using the equation proposed by Bonazza *et al.* (2009) (Equation 3). This equation incorporates factors such as the Young's modulus (E), the coefficient of thermal expansion (α), Poisson's ratio (ν), and the daily air temperature range (daily ΔT_{air} = DTR), with an additional 20 °C to account for

the surface temperature. Specifically, it assumes that the daily air temperature range on the marble's surface is 20 °C higher than the daily air temperature range. Equation 3 is used to assess the risk of thermal stress under future climate change scenarios, given the expected rise in temperatures.

$$\sigma_t = E \cdot \alpha \cdot (\text{daily } \Delta T_{\text{air}} + 20 \text{ } ^\circ\text{C}) / (1 - \nu) \quad (3)$$

In this study we used the equation by Bonazza *et al.* (2009), who applied it in a Mediterranean region (Malta) like Thessaloniki and examined Carrara marble, which is primarily calcite-based –just like the marble of the Arch of Galerius. Accordingly, we assume $E=70 \text{ GPa}$, $\alpha=8 \cdot 10^{-6} \text{ K}^{-1}$, and $\nu=0.25$. The daily temperature outputs from the WRF model at 1 km were then used to calculate the maximum and minimum daily temperatures, estimate the mean daily DTR (or ΔT_{air} in Equation 3), and compute the σ_t value for each period.

3. Results and discussion

3.1. Analysis of future climate trends and implications for the monument

Table 3 presents the results of future temperature trends under the RCP4.5 scenario, using ETCCDI indices.

According to the trend analysis, the RCA4 regional model shows a marked decrease in frost days (FD) compared to the 1971–2000 baseline period. Their largest percentage reduction occurs between 2021–2050, and although the decrease remains significant by the end of the century (2071–2100), it is not as pronounced as in the earlier period. Ice days (ID) disappear over the long-term. The high percentage change in ID arises from the extremely small number of such days in the historical record. This trend toward fewer frost days reflects milder winters and fewer extreme cold events, as noted by Katopodis *et al.* (2020), Georgoulas *et al.* (2022), and Ioannidis *et al.* (2024). The diurnal temperature range (DTR) increases slightly – values of 0.09 and 0.10 may seem small but align with the overall warming trend.

The annual maximum of the daily maximum temperatures (TXx) increases significantly, especially toward the end of the century, suggesting more frequent and intense heat events. Its standard deviation (SD) also increases slightly yet steadily, indicating a greater variability in the future. The interquartile range (IQR) of TXx grows more

noticeably during 2071–2100, pointing to a wider spread in the central 50% of extreme temperature values.

The annual minimum of the daily minimum temperatures (TNn) rises, showing that the coldest temperatures are becoming less cold, consistent with Politi *et al.* (2023). The percentage change for TNn is negative because its baseline (reference) value was below zero. Meanwhile, the SD of TNn exhibits a substantial percentage increase, indicating that the coldest days and nights will have greater variability. Although absolute minimum temperatures (TNn) generally increase, the pronounced rise in SD suggests these low values will be more spread out around their mean. Finally, the IQR of TNn decreases by mid-century (indicating more clustered extremely cold values), but returns to positive values at century's end, signaling a slight widening of the distribution of the lowest temperatures.

Overall, both cold and hot temperature extremes become warmer, particularly at the cold end, and in many cases more variable – features characteristic of how climate change impacts extreme events.

Table 3. Temperature indices trends under the RCP4.5 scenario for the near future (2021–2050) and the far future (2071–2100), based on the reference period 1971–2000

Indices	Units	Difference (2021–2050 vs. 1971–2000)	Difference (2071–2100 vs. 1971–2000)	% Change 2021–2050	% Change 2071–2100
FD	days	-11.53	-6.57	-38.65	-21.91
ID	days	-0.05	-1.08	-14.29	-308.57
TXx	°C	2.33	2.55	5.81	6.35
TXx SD	°C	0.12	0.10	7.89	6.57
TXx IQR	°C	0.08	0.32	3.39	13.56
TNn	°C	0.34	0.79	-10.59	-24.61
TNn SD	°C	0.98	0.87	54.14	48.07
TNn IQR	°C	-1.03	0.07	-52.02	3.54
DTR	°C	0.09	0.10	0.77	0.85

Rising temperatures and the substantial decrease in extremely cold days have various implications for the Arch of Galerius monument. Higher maximum temperatures increase thermal stress on the marble. Even a slight increase in the diurnal temperature range (DTR) signifies greater fluctuations between day and night, which in turn intensifies thermal stress – especially in porous materials like calcite marble, known to be extremely sensitive to ambient temperature variations (Åkesson *et al.*, 2006; Luque *et al.*, 2011). Repeated expansion and contraction can lead to the formation or widening of cracks, thereby accelerating deterioration (Blavier *et al.*, 2023).

Although the significant reduction in frost days (FD) and the near elimination of ice days (ID) may limit freeze-thaw phenomena – which mechanically affect the structure of marble – periods of ice days (though less frequent) could become more intense locally, particularly as variability increases at the colder extremes (see SD). An increase in SD and IQR (especially at higher temperature extremes) indicates more unstable thermal loads on the material. Sudden transitions between extremely hot and cooler phases can intensify mechanical stress. Moreover, on the

frost days, there is greater variability, meaning that certain (rarer) cold spells might still be severe enough to cause cracking. Therefore, temperature remains a critical factor in the deterioration of marble monuments.

3.2. Dynamical downscaling and implications for the monument

Dynamical downscaling is performed to study temperature at a higher spatial resolution, considering microclimatic conditions and thereby making temperature assessments more reliable. The use of high-resolution models (1 km) enables a more accurate depiction of local climate characteristics and microclimatic phenomena (Ascenso *et al.*, 2024). Below, we compare several future months to illustrate the trend in temperature variability.

In **Figure 3**, the overall trend shows that most points – specifically 75% of the June days examined (June 5–25) – lie above the reference line $y = x$. This indicates that on most of these days in 2048, the DTR is higher compared to 2023. More precisely, most 2048 DTR values range from about 7 °C to 9 °C, whereas in 2023 they range from 3 °C to 8 °C, pointing to lower variability. Only a few days show

a smaller 2023 DTR, suggesting that conditions are not entirely uniform for all dates. The predominance of higher daily variability in 2048 compared to 2023 signifies more intense thermal fluctuations in the future, linked to climate change impacts, with more extreme daytime maximum temperatures on day and cooler nighttime minimum temperatures.

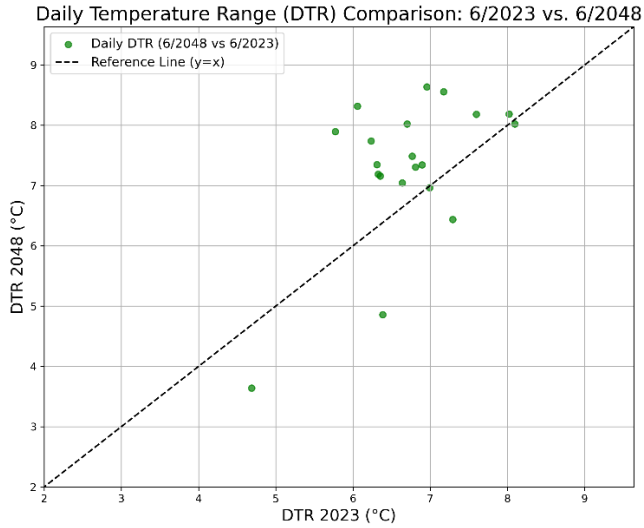


Figure 3. Scatter plot showing the daily temperature range from June 5 to June 25 in 2023 compared to 2048

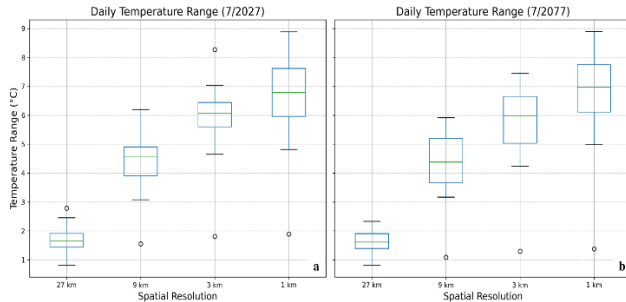


Figure 4. Box plot illustrating the daily temperature range for the spatial resolutions of 27 km, 9 km, 3 km, and 1 km for July (a) 2025 and (b) 2077

Figure 4 highlights the influence of climate change and the importance of spatial resolution in future temperature projections. The DTR for July 2077 (**Figure 4b**) is higher than that for July 2027 (**Figure 4a**) at all spatial resolutions, confirming the findings from the previous figure (**Figure 3**) that DTR increases over time, reflecting potential climate change impacts with more pronounced day-night temperature differences. In both years, the 1 km resolution displays significantly higher DTR compared to the lower resolutions (27 km, 9 km). This is because higher-resolution data captures local temperature variations more accurately (Ascenso *et al.*, 2024), whereas coarser resolutions (e.g., 27 km) smooth out temperatures due to their larger grid size. Qiu *et al.* (2020) demonstrate the strong added value of high resolution (5 km) in long-term climate modeling, as it improves the simulation of extreme temperatures and local details through a more accurate representation of topography.

3.3. Temperature impact on the monument's material

Thermal stress (σ_t) was calculated using Equation 3 for specific future years in July – namely 2050, 2077, and

2092. The difference between these future years and the baseline year of 2027 was then computed. **Figure 5** shows maps depicting the differences in thermal stress for these future periods compared to July 2027. The results indicate that thermal stress is higher in July 2092 by 1.5% compared to July 2027, followed by July 2050 (1.45%) and July 2077 (0.65%). This means that, over time, DTR (diurnal temperature range) does not necessarily increase in a strictly linear manner; it can show either upward or downward trends. Nonetheless, the overall trend points to a future increase in DTR (see Subsection 3.1). In absolute terms, a 1.5% increase over 65 years (2092–2027) may not seem large. However, given that the monument was in poor conservation condition for many years (Samara *et al.*, 2020), meaning it had already suffered some degree of deterioration, even a small percentage rise in thermal stress can accelerate marble decay or raise the likelihood of cracks. Moreover, because this material is of high cultural and historical value, such an increase can be particularly significant. This increase is based on the moderate RCP4.5 scenario; thus, if a more adverse scenario (e.g., RCP8.5) were to occur, thermal stress would be even greater. Finally, in archaeological terms, 65 years is a brief period, and even a minor increase in stress can have a cumulative effect over time.

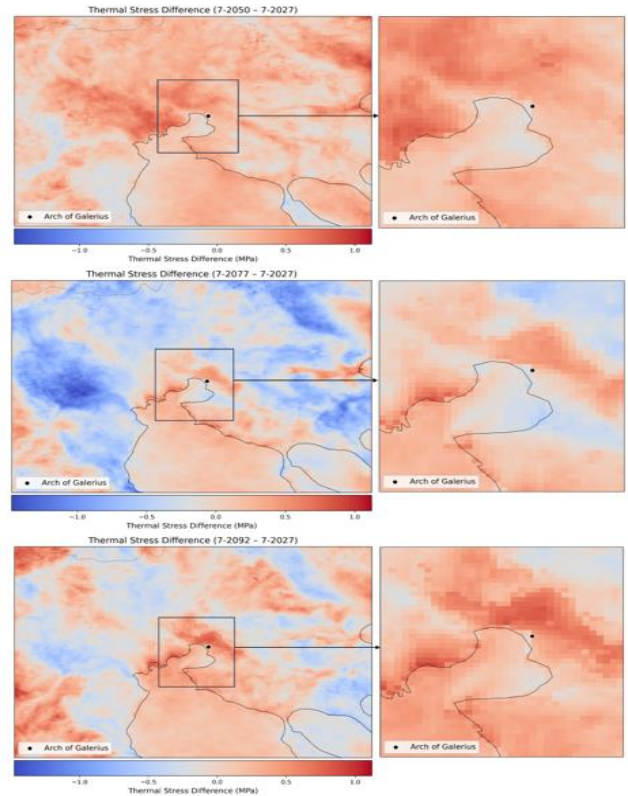


Figure 5. Difference in thermal stress (σ_t) for July in the future years 2050, 2077, and 2092 compared to July 2027, at a 1 km resolution

The maps presented below are derived from the WRF model at a 1 km spatial resolution. High-resolution climate simulations yield more pronounced and detailed outcomes, as illustrated in **Figure 5**, where thermal stress is notably greater between 7/2092 and 7/2027. Employing this level of resolution enhances the precise analysis of climate parameters, allowing for accurate microclimatic

simulations and more reliable assessments of deterioration risk. Moreover, it provides a clearer understanding of the impacts of climate change on sites housing cultural heritage, such as the monument of the Arch of Galerius in Thessaloniki.

4. Conclusions

This study confirmed the significant impact of climate change on temperature and thermal stress experienced by cultural heritage monuments, focusing on the Arch of Galerius in Thessaloniki, Greece. High-resolution simulations (WRF-ARW) and future trend analyses based on EURO-CORDEX data under the RCP4.5 scenario revealed an increase in both temperature and diurnal temperature range (DTR) in the future periods (2021-2050 and 2071-2100) compared to the reference period (1971-2000).

Our analysis showed a 75% increase in the number of days with higher DTR in June 2048 compared to June 2023, alongside a 1.5% rise in thermal stress in July 2092 relative to July 2027. These findings are in line with Bonazza *et al.* (2009), who predict that in the Mediterranean region, the number of events where thermal stress exceeds 20 MPa could increase by up to 50 events per year, with total values potentially surpassing 300 events per year in the future. Together, these results underscore the critical impact of climate change on the thermal performance of marble, highlighting the need for localized assessments and adaptive conservation strategies for cultural heritage. The use of high spatial resolution (1 km) uncovered notably higher DTR values, capturing local variability more accurately than lower resolutions (27 km and 9 km). Guo *et al.* (2018) emphasize that the higher resolution of RCMs provides more detailed spatial information compared to GCMs, which are unable to capture these fine-scale features to the same extent – a factor that is crucial for the more accurate simulation of indices such as the DTR. However, Avila-Diaz *et al.* (2020) perform dynamical downscaling with various high-resolution models and emphasize that while high resolution enhances the simulation of physical processes, it is not the sole and most critical factor determining model performance, as model physics and downscaling procedures also play significant roles. These findings highlight the importance of local temperature fluctuations for the structural integrity of marble materials, as elevated DTR intensifies thermal stresses that can lead to cracking, microstructural failures, and accelerated deterioration of monuments.

While the study provides a robust methodological framework for assessing the impacts of climate change on monuments, several limitations should be noted. First, the analysis was confined to the RCP4.5 scenario, which, although realistic, does not capture the full spectrum of potential future climate conditions. Second, the simulation periods, though extensive, may not fully represent extreme events that could occur outside the selected intervals. Third, the focus on temperature and DTR excludes other important climatic factors such as humidity, precipitation, and pollution, which also contribute to material degradation. Additionally,

uncertainties inherent in regional climate models and input data may affect the precision of the projections.

Considering these limitations, future research should expand the framework by incorporating additional climatic variables (e.g., humidity, precipitation, and pollution) and employing an ensemble of Regional Climate Models (RCMs) to better capture uncertainty and variability. Moreover, extending the simulations to include critical future periods and other geographical areas will be essential for a more comprehensive risk assessment. Upcoming researchers are encouraged to explore the integration of these enhanced climate impact assessments with advanced conservation strategies, potentially incorporating real-time monitoring systems and adaptive maintenance practices, to ensure the long-term preservation of cultural heritage monuments under rapidly changing climatic conditions.

Acknowledgments

This work utilized the computational resources of the supercomputer BwUniCluster 2.0 located at the Karlsruhe Institute of Technology (KIT), which last accessed on November 15, 2024. The authors acknowledge support by the state of Baden-Württemberg through bwHPC. Also, we acknowledge the European Coordinated Regional Climate Downscaling Experiment (EURO-CORDEX) for providing the meteorological data used in estimating future climate trends. Finally, we acknowledge the European Centre of Medium-Range Weather Forecasts (ECMWF) – Copernicus Climate Change Service (C3S) for providing the dataset used to initialize the historical WRF-ARW simulations. We also thank the NCAR CESM Global Bias-Corrected CMIP5 Output to Support WRF/MPAS Research for providing the initial and boundary conditions for the future WRF simulations.

References

- Åkesson U., Lindqvist J. E., Schouenborg B. and Grellk B. (2006), Relationship between microstructure and bowing properties of calcite marble claddings. *Bulletin of Engineering Geology and the Environment*, **65**(1), 73–79. <https://doi.org/10.1007/s10064-005-0026-x>
- Ascenso A., Augusto B., Coelho S., Menezes I., Monteiro A., Rafael S., Ferreira J., Gama C., Roebeling P. and Miranda A. I. (2024), Assessing Climate Change Projections through High-Resolution Modelling: A Comparative Study of Three European Cities. *Sustainability*, **16**(17), 7276. <https://doi.org/10.3390/su16177276>
- Avila-Diaz A., Abrahão G., Justino F., Torres R. and Wilson A. (2020), Extreme climate indices in Brazil: evaluation of downscaled earth system models at high horizontal resolution. *Climate Dynamics*, **54**(11–12), 5065–5088. <https://doi.org/10.1007/s00382-020-05272-9>
- Blavier C. L. S., Huerto-Cardenas H. E., Aste N., del Pero C., Leonforte F. and della Torre S. (2023), Adaptive measures for preserving heritage buildings in the face of climate change: A review. *Building and Environment*, **245**. <https://doi.org/10.1016/j.buildenv.2023.110832>
- Bonazza A., Sabbioni C., Messina P., Guaraldi C. and De Nuntiis P. (2009), Climate change impact: Mapping thermal stress on Carrara marble in Europe. *Science of the Total Environment*,

- 407(15), 4506–4512. <https://doi.org/10.1016/j.scitotenv.2009.04.008>
- Castorina G., Caccamo M. T., Insinga V., Magazù S., Munaò G., Ortega C., Sempredello A. and Rizza U. (2022), Impact of the Different Grid Resolutions of the WRF Model for the Forecasting of the Flood Event of 15 July 2020 in Palermo (Italy). *Atmosphere*, **13**(10). <https://doi.org/10.3390/atmos13101717>
- Covey-Crump S. J. and Rutter E. H. (1989), Thermally-induced grain growth of calcite marbles on Naxos Island, Greece. *Contributions to Mineralogy and Petrology*, **101**, 69–86. <https://doi.org/10.1007/BF00387202>
- Georgoulas A. K., Akritidis D., Kalisoras A., Kapsomenakis J., Melas D., Zerefos C. S. and Zanis P. (2022), Climate change projections for Greece in the 21st century from high-resolution EURO-CORDEX RCM simulations. *Atmospheric Research*, **271**. <https://doi.org/10.1016/j.atmosres.2022.106049>
- Guo J., Huang G., Wang X., Li Y. and Lin Q. (2018), Dynamically-downscaled projections of changes in temperature extremes over China. *Climate Dynamics*, **50**(3–4), 1045–1066. <https://doi.org/10.1007/s00382-017-3660-7>
- Hersbach H., Bell B., Berrisford P., Biavati G., Horányi A., Muñoz Sabater J., Nicolas J., Peubey C., Radu R., Rozum I., Schepers D., Simmons A., Soci C., Dee D., Thépaut J.-N. (2023a), ERA5 hourly data on pressure levels from 1940 to present. *Copernicus Climate Change Service (C3S) Climate Data Store (CDS)*, <https://doi.org/10.24381/cds.bd0915c6>. Accessed on 13/03/2025.
- Hersbach H., Bell B., Berrisford P., Biavati G., Horányi A., Muñoz Sabater J., Nicolas J., Peubey C., Radu R., Rozum I., Schepers D., Simmons A., Soci C., Dee D., Thépaut J.-N. (2023b), ERA5 hourly data on single levels from 1940 to present. *Copernicus Climate Change Service (C3S) Climate Data Store (CDS)*, <https://doi.org/10.24381/cds.adbb2d47>. Accessed on 13/03/2025.
- Ioannidis C., Verykokou S., Soile S., Istrati D., Spyarakos C., Sarris A., Akritidis D., Feidas H., Georgoulas A. K., Tringa E., Zanis P., Georgiadis C., Martino S., Feliziani F., Marmoni G. M., Cerra D., Ottinger M., Bachofer F., Anastasiou A., ... Anyfantis G. C. (2024), Safeguarding Our Heritage—The TRIQUETRA Project Approach. *Heritage*, **7**(2), 758–793. <https://doi.org/10.3390/heritage7020037>
- Jacob D., Teichmann C., Sobolowski S., Katragkou E., Anders I., Belda M., Benestad R., Boberg F., Buonomo E., Cardoso R. M., Casanueva A., Christensen O. B., Christensen J. H., Coppola E., de Cruz L., Davin E. L., Dobler A., Domínguez M., Fealy R., and Wulfmeyer V. (2020), Regional climate downscaling over Europe: perspectives from the EURO-CORDEX community. *Regional Environmental Change*, **20**(2). <https://doi.org/10.1007/s10113-020-01606-9>
- Katopodis T., Markantonis I., Politi N., Vlachogiannis D. and Sfetsos, A. (2020), High-resolution solar climate atlas for Greece under climate change using the weather research and forecasting (WRF) model. *Atmosphere*, **11**(7). <https://doi.org/10.3390/ATMOS11070761>
- Koch A. and Siegesmund S. (2004), The combined effect of moisture and temperature on the anomalous expansion behaviour of marble. *Environmental Geology*, **46**(3–4), 350–363. <https://doi.org/10.1007/s00254-004-1037-9>
- Luque A., Ruiz-Agudo E., Cultrone G., Sebastián E. and Siegesmund S. (2011), Direct observation of microcrack development in marble caused by thermal weathering. *Environmental Earth Sciences*, **62**(7), 1375–1386. <https://doi.org/10.1007/s12665-010-0624-1>
- Malaga-Starzec K., Lindqvist J. E. and Schouenborg, B. (2002), Experimental study on the variation in porosity of marble as a function of temperature. Geological Society, London, *Special Publications*, **205**, 81–88. <https://doi.org/10.1144/GSL.SP.2002.205.01.07>
- Monaghan A. J., Steinhoff D. F., Bruyere C. L. and Yates D. (2014), NCAR CESM Global Bias-Corrected CMIP5 Output to Support WRF/MPAS Research, Research Data Archive at the National Center for Atmospheric Research, *Computational and Information Systems Laboratory*, <https://doi.org/10.5065/D6DJ5CN4>. Accessed on 13/03/2025.
- Politi N., Nastos P. T., Sfetsos A., Vlachogiannis D. and Dalezios N. R. (2018), Evaluation of the AWR-WRF model configuration at high resolution over the domain of Greece. *Atmospheric Research*, **208**, 229–245. <https://doi.org/10.1016/j.atmosres.2017.10.019>
- Politi N., Vlachogiannis D., Sfetsos A. and Nastos P. T. (2023), High resolution projections for extreme temperatures and precipitation over Greece. *Climate Dynamics*, **61**(1–2), 633–667. <https://doi.org/10.1007/s00382-022-06590-w>
- Qiu L., Im E. S., Hur J. and Shim K. M. (2020), Added value of very high resolution climate simulations over South Korea using WRF modeling system. *Climate Dynamics*, **54**(1–2), 173–189. <https://doi.org/10.1007/s00382-019-04992-x>
- Rees R. (1993), Images and Image: A Re-Examination of Tetrarchic Iconography. *Greece and Rome*, **40**(2), 181–200. <https://doi.org/10.1017/S0017383500022774>
- Samara C., Melfos V., Kouras A., Karali E., Zacharopoulou G., Kyranoudi M., Papadopoulou L. and Pavlidou E. (2020), Morphological and geochemical characterization of the particulate deposits and the black crust from the Triumphal Arch of Galerius in Thessaloniki, Greece: Implications for deterioration assessment. *Science of the Total Environment*, **734**. <https://doi.org/10.1016/j.scitotenv.2020.139455>
- Sassoni E. and Franzoni E. (2014), Influence of porosity on artificial deterioration of marble and limestone by heating. *Applied Physics A: Materials Science and Processing*, **115**(3), 809–816. <https://doi.org/10.1007/s00339-013-7863-4>
- Schulzweida U. (2023), CDO User Guide, Version 2.3.0. <https://code.mpimet.mpg.de/projects/cdo/embedded/cdo.pdf>
- Sesana E., Gagnon A. S., Bonazza A. and Hughes J. J. (2020), An integrated approach for assessing the vulnerability of World Heritage Sites to climate change impacts. *Journal of Cultural Heritage*, **41**, 211–224. <https://doi.org/10.1016/j.culher.2019.06.013>
- Siegesmund S., Menningen J. and Shushakova V. (2021), Marble decay: towards a measure of marble degradation based on ultrasonic wave velocities and thermal expansion data. *Environmental Earth Sciences*, **80**(11). <https://doi.org/10.1007/s12665-021-09654-y>
- Skamarock W. C., Klemp J. B., Dudhia J., Gill D. O., Liu Z., Berner J., Wang W., Powers J. G., Duda M. G., Barker D. M. and Huang X.-Y. (2019), A Description of the Advanced Research WRF Model Version 4. <http://library.ucar.edu/research/publish-technote>

- Stevens B., Giorgetta M., Esch M., Mauritsen T., Crueger T., Rast S., Salzmann M., Schmidt H., Bader J., Block K., Brokopf R., Fast I., Kinne S., Kornblueh L., Lohmann U., Pincus R., Reichler T. and Roeckner E. (2013), Atmospheric component of the MPI-M earth system model: ECHAM6. *Journal of Advances in Modeling Earth Systems*, **5**(2), 146–172. <https://doi.org/10.1002/jame.20015>
- Subramanian S., Geetha Rani K., Madhavan M. and Rajendran S. (2024), An automatic data-driven long-term rainfall prediction using Humboldt squid optimized convolutional residual attentive gated circulation model in India. *Global Nest Journal*, **26**(10). <https://doi.org/10.30955/gnj.06421>
- Surendran R., Alotaibi Y. and Subahi A. F. (2023), Wind Speed Prediction Using Chicken Swarm Optimization with Deep Learning Model. *Computer Systems Science and Engineering*, **46**(3), 3371–3386. <https://doi.org/10.32604/csse.2023.034465>
- Surendran R., Tamilvizhi T. and Lakshmi S. (2021), Integrating the meteorological data into a smart city service using cloud of things (CoT). Emerging Technologies in Computing: 4th EAI/IAER International Conference, ICETIC 2021, Virtual Event, August 18–19, **395**. <https://doi.org/10.1007/978-3-030-90016-8>
- Thomson A. M., Calvin K. v., Smith S. J., Kyle G. P., Volke A., Patel P., Delgado-Arias S., Bond-Lamberty B., Wise M. A., Clarke L. E. and Edmonds J. A. (2011), RCP4.5: A pathway for stabilization of radiative forcing by 2100. *Climatic Change*, **109**(1), 77–94. <https://doi.org/10.1007/s10584-011-0151-4>
- Tringa E. and Tolika K. (2023), Analysis of the Outdoor Microclimate and the Effects on Greek Cultural Heritage Using the Heritage Microclimate Risk (HMR) and Predicted Risk of Damage (PRD) Indices: Present and Future Simulations. *Atmosphere*, **14**, 663. <https://doi.org/10.3390/atmos14040663>
- van Vuuren D. P., Edmonds J., Kainuma M., Riahi K., Thomson A., Hibbard K., Hurtt G. C., Kram T., Krey V., Lamarque J. F., Masui T., Meinshausen M., Nakicenovic N., Smith S. J. and Rose S. K. (2011), The representative concentration pathways: An overview. *Climatic Change*, **109**(1), 5–31. <https://doi.org/10.1007/s10584-011-0148-z>
- Zhang X., Alexander L., Hegerl G. C., Jones P., Tank A. K., Peterson T. C., Trewin B. and Zwiers F. W. (2011), Indices for monitoring changes in extremes based on daily temperature and precipitation data. *Wiley Interdisciplinary Reviews: Climate Change*, **2**(6), 851–870. <https://doi.org/10.1002/wcc.147>